

Published in final edited form as:

J Biomed Mater Res A. 2009 July ; 90(1): 70–81. doi:10.1002/jbm.a.32056.

Bioactive interpenetrating polymer network hydrogels that support corneal epithelial wound healing

David Myung^{1,2}, Nabeel Farooqui¹, Luo Luo Zheng¹, Wongun Koh³, Jaan Noolandi^{1,2}, Jennifer R. Cochran⁴, Curtis W. Frank², and Christopher N. Ta^{1,#}

¹ Department of Ophthalmology, Stanford University School of Medicine, 300 Pasteur Drive, Stanford, CA 94305–5080

² Department of Chemical Engineering, Stanford University, 381 North-South Mall, Stauffer III, Stanford, CA 94305

³ Department of Chemical Engineering, Yonsei University, 134 Shinchon-dong, Seodaemun-ku, Seoul 120–749, South Korea

⁴ Department of Bioengineering, Stanford University, 318 Campus Drive, Clark Center, Stanford, CA 94305

Abstract

We describe the development and characterization of collagen-coupled poly(ethylene glycol)/poly(acrylic acid) (PEG/PAA) interpenetrating polymer network hydrogels. Quantitative amino acid analysis and FITC-labeling of collagen were used to determine the amount and distribution of collagen on the surface of the hydrogels. The bioactivity of the coupled collagen was detected by a conformation-specific antibody and was found to vary with the concentration of collagen reacted to the photochemically functionalized hydrogel surfaces. A wound healing assay based on an organ culture model demonstrated that this bioactive surface supports epithelial wound closure over the hydrogel but at a decreased rate relative to sham wounds. Implantation of the hydrogel into the corneas of live rabbits demonstrated that epithelial cell migration is supported by the material, although the rate of migration and morphology of the epithelium were not normal. The results from the study will be used as a guide toward the optimization of bioactive hydrogels with promise in corneal implant applications such as a corneal onlay and an artificial cornea.

1. INTRODUCTION

Over 10 million people worldwide are blind due to corneal disease. Corneal transplantation is highly effective at treating this condition, but is limited in worldwide distribution due to both economic and cultural factors^{1–3}. Artificial corneas offer an alternative treatment that has potential for widespread, cost-effective distribution to patients who are blind due to corneal disease. These devices come in two general categories: tissue-engineered corneas and synthetic corneal prostheses (keratoprotheses)³. While tissue-engineered constructs containing functional corneal cells are extremely promising, they are still in preclinical development^{3–5}. A number of keratoprotheses, on the other hand, are now available to restore sight to individuals with severe blindness refractory to standard transplantation^{2,6–9}. However, these devices are still only reserved for cases in which human donor transplants fail.

#Author to whom correspondence should be addressed. Department of Ophthalmology, Stanford University, 900 Blake Wilbur Drive, W3036, Stanford, CA 94304–5353. cta@stanford.edu, Phone: (650) 498–4791, Fax: (650) 498–4222.

One of the most formidable challenges in the development of a keratoprosthesis equivalent to donor corneas is epithelialization of the implant surface. While the positive outcomes of current keratoprostheses such as the Boston, Osteo-Odonto, and AlphaCor keratoprostheses demonstrate that epithelialization is not a requirement for prosthetic vision^{1-3,6,7,10-14}, it has been argued that epithelial coverage can increase retention rates and minimize risk of infections by serving as a barrier to microbial contamination and debris^{1,3}. A number of investigators have made progress in this regard^{4,5,15-22}, but to date, a keratoprosthesis that supports surface epithelialization has yet to become a clinical reality in human patients.

Corneal epithelial wound healing is a complex process involving interactions among migrating cells, their underlying matrix, and available nutrients and growth factors^{23,24}. Two main elements are required to support epithelialization on a corneal device: (1) high bulk permeability to allow passage of glucose and other nutrients to the overlying cells, and (2) a surface that mimics the extracellular matrix of the corneal bed to encourage epithelial adhesion and migration. Inspired by the “double networks” described by Gong and coworkers²⁵, we have developed interpenetrating polymer networks (IPNs) based on poly(ethylene glycol) (PEG) and poly(acrylic acid) (PAA) (Figure 1) and have demonstrated that they exhibit “biomimetic” mechanical properties and high permeability to glucose²⁶⁻²⁸. PEG and PAA are hydrophilic polymers which have found favor in a variety of biomedical applications, including drug-delivery and biosensors, due to their hydrophilicity and biocompatibility²⁹⁻³¹. While many polymer combinations phase separate and become opaque, PEG and PAA are highly miscible with each other and form optically transparent blends, a feature of utmost importance to a corneal implant.

Unfortunately, the intrinsic resistance of PEG and PAA to protein adsorption also renders these materials resistant to cell adhesion (Figure 2a), which is an essential component for many tissue engineering applications, including artificial corneas and corneal onlays. A biointegrable keratoprosthesis based on PEG and PAA polymers must be modified on its anterior surface to encourage the overgrowth of epithelial cells. Moreover, it must support epithelialization via peripheral migration from adjacent host tissue. This requires relatively robust coverage of cell adhesion-promoting biomolecules to provide a matrix upon which an epithelium can migrate and grow. Site-specific surface modification of our intrinsically protein-resistant PEG/PAA material with extracellular matrix proteins is an attractive strategy because it will encourage cell growth in a defined region without compromising the materials’ intrinsic passivity in other regions. Methods such as gamma-ray irradiation, plasma, or glow discharge treatment have been studied extensively as techniques for altering the surface chemistry of materials to yield reactive functional groups for subsequent linkages. Such techniques make possible the creation of self-assembled monolayers, adsorption of polymers from solution, and the growth of polymers at the surface *in situ* through surface-initiated polymerization. However, a common feature among these and other techniques is the need for reactive sites on the surface to which molecules can bind. Often times, no defined surface chemistry is available, because the surface is either too inert or too heterogeneous³². These limitations have created a need for more versatile methods that are independent of the materials to be coupled.

In this paper, we use photoreactive, heterobifunctional crosslinker (5-azido-2-nitrobenzoyloxy-N-hydroxysuccinimide ester) to covalently tether collagen type I, the predominant extracellular matrix protein in the cornea, to PEG/PAA IPN hydrogels, to create a biosynthetic polymer supportive of surface cell growth (Figure 2b). Previously, Matsuda and coworkers demonstrated the use of photoreactive phenyl azides for the site-specific coupling of cell adhesion-promoting proteins to polymeric substrates³³⁻³⁵. The heterobifunctional crosslinker contains a light-sensitive azide moiety that reacts rapidly with polymer surfaces and an N-hydroxysuccinimide moiety that reacts with free amino groups

of the collagen protein. In previous work, we demonstrated that primary corneal epithelial cells cultured from rabbit eyes could be grown to confluence on hydrogels coupled with collagen type I with this technique²⁷. In this study, we explore this chemical attachment procedure in more detail through visualization, quantification, and evaluation of the conformational integrity of the bound collagen type I. We then evaluate these collagen-tethered hydrogels for their capacity to support the migration of corneal epithelial cells, first through an *in vitro* organ culture assay and then through a small number of *in vivo* implantations in live rabbit corneas. These experiments validate our crosslinking strategy as a viable approach to control the presentation of bioactive proteins at hydrogel surfaces, and show that this strategy applied to PEG/PAA hydrogels provides a promising approach to prosthetic epithelialization.

2. MATERIALS AND METHODS

2.1 Hydrogel Synthesis

PEG/PAA interpenetrating networks were synthesized by a two-step sequential network formation technique based on UV-initiated free radical polymerization. A precursor solution for the first network was composed of 50% w/w purified PEG-diacrylate (PEG-DA, made by methods described elsewhere²⁶ from PEG MW 8000) dissolved in deionized water along with 2-hydroxy-2-methyl propiophenone, a UV-sensitive free-radical initiator, at a concentration of 1% with respect to the PEG-DA macromonomer. The solution was cast into a glass/Teflon mold, covered with a glass plate, and reacted under a UV light source at room temperature. The mold consisted of Teflon spacers placed between glass plates. Upon UV exposure, the precursor solution underwent free-radical induced gelation and became insoluble in water. The resulting transparent PEG hydrogel was gently peeled off the glass with a metal spatula and had a smooth, homogeneous surface. To incorporate the second network, the hydrogel was removed from the mold and immersed in a 50% v/v acrylic acid solution with 1% v/v (with respect to the monomer) 2-hydroxyl-2-methyl propiophenone as the photoinitiator, and 1% v/v (with respect to the monomer) triethylene glycol dimethacrylate as the crosslinking agent for 24 h at room temperature. The swollen gel was then placed back between glass plates along with Teflon spacers and exposed to the UV source. In this way, the acrylic acid monomers were polymerized within the polyethylene glycol network to form an interpenetrating polymer network structure. Following synthesis, the PEG/PAA hydrogels were washed extensively in Dulbecco's phosphate buffered saline (DPBS) with repeated solvent exchanges at 37 C for 5 days to remove any unreacted components and to facilitate equilibrium swelling. The water content of the hydrogels increased from 80% to about 90% after equilibration in DPBS.

2.2. Swelling Measurements

The water content of the hydrogels was evaluated by measuring their swollen and dry weights. Dried hydrogels were weighed and immersed in water. At regular intervals, the swollen gels were lifted, patted dry, and weighed until equilibrium was attained. The percentage of equilibrium water content (WC) was calculated from the swollen and dry weights of the hydrogel:

$$WC = \frac{W_s - W_d}{W_s} \times 100 \quad (1)$$

where W_s and W_d are the weights of swollen and dry hydrogel, respectively.

2.3 Surface Modification

Substituted phenyl azides react with light (250–320 nm) to generate aromatic nitrenes, which insert into a variety of covalent bonds. Varying amounts (0.5–5 mg) of 5-azido-2-nitrobenzoic acid N-hydroxysuccinimide ester in 1 mL of N,N-dimethylformamide (DMF) were evenly spread over partially dried hydrogel surfaces; the DMF solution was then evaporated by air-drying and exposed to UV for 5 min. Upon UV irradiation, the phenyl azide group reacts to form covalent bonds with the hydrogel surface. Irradiated surfaces were thoroughly rinsed with solvent to remove any unreacted crosslinker from the surface. All PEG/PAA hydrogels (both functionalized and unfunctionalized) were sterilized under UV light in phosphate buffered saline for 1 h and then placed in tissue culture plates in preparation for subsequent characterization studies. Sterilized hydrogels were swelled to equilibrium and washed extensively by solvent exchange for a minimum of five days in Dulbecco's phosphate buffered saline supplemented with antibiotic and antimycotic (Invitrogen, Carlsbad, CA).

Alternatively, surface-functionalized hydrogels were incubated with varying concentrations of collagen type I (Inamed Biomaterials, Fremont, CA) in phosphate buffered saline at 37°C for 16 h during which primary amines react with the N-hydroxysuccinimide groups to form covalent linkages.

2.4 Cell Seeding

A rabbit corneal cell line (ATCC #CCL60) was used to determine the ability of the hydrogels to support cell adhesion and growth. The cells were cultured in Eagle's Minimum Essential Media (ATCC 30–2003) supplemented with 10% fetal bovine serum (Invitrogen, Carlsbad, CA) at 37 C and 5% CO₂ and seeded on samples of unmodified and collagen-modified hydrogels at a concentration of 1×10^5 cells/ml. The cells were visualized using a Nikon inverted phase contrast microscope, and images were captured using Metamorph software.

2.5 Surface Characterization

The distribution of collagen on the hydrogel surface was assessed qualitatively by visualization of fluorescein isothiocyanate (FITC)-labeled collagen type I bound to the hydrogel surface using an epifluorescent inverted phase contrast microscope. Briefly, 1 mL of a 0.1% w/v FITC-labeled collagen type I (from bovine skin, Sigma-Aldrich, St. Louis, MO) solution was reacted with the functionalized hydrogels at 37°C for 16 hours. The functionalized hydrogels were reacted with 1 mL of a 0.1% w/v FITC-labeled collagen type I (from bovine skin, Sigma-Aldrich, St. Louis, MO) solution at 37°C for 16 h. The hydrogel surface was rinsed three times with phosphate buffered saline and then examined with an inverted phase contrast microscope under fluorescence. The same process was carried out using non-fluorescing collagen type I from bovine skin (Inamed Biomaterials, Fremont, CA) and then evaluated by quantitative amino acid analysis. Briefly, the collagen-coated samples were hydrolyzed in 6N HCl and then amino acid residues were detected using a Model L-8800 Amino Acid Analyzer (Hitachi High Technologies America, San Jose, CA) at the Molecular Structure Facility at UC Davis (Davis, CA).

2.6 ELISA Surface Bioactivity Assay

The amount of collagen type retaining its native conformation after coupling to hydrogel surfaces was determined using a modified ELISA-based protocol¹⁶. Hydrogel samples were cut into discs 6.0 mm in diameter and then placed at the bottoms of the wells of a microtiter plate (MaxiSorp, Nunc). Unreacted hydrogel and microplate binding sites were blocked with phosphate buffered saline containing 3% bovine serum albumin. Hydrogel-collagen surfaces

were washed with phosphate buffered saline containing 0.05% Triton-X100 (PBST) and incubated in 2 µg/ml of a conformation-specific collagen type I antibody (monoclonal antibody COL-1, Sigma-Aldrich) for 2 h at room temperature. Wells were washed with PBST and then incubated in a 1:4000 dilution of horseradish peroxidase-conjugated secondary antibody (Sigma-Aldrich) for 1 h at room temperature. After final washes with PBST, 1 mg/ml of o-phenylenediamine dihydrochloride was added to produce a colorimetric signal that could be measured at 450 nm using a microplate reader (BioTek, Winooski, VT). Hydrogel-coupled collagen type I proteins that have first been denatured by boiling were used for comparison with native, biologically active protein. Relative amounts of bioactive collagen on the surface of the hydrogels were determined by comparison with a standard curve of microtiter plate-coated collagen type I that was adsorbed for 2 hours at 37°C.

2.7 Bovine Organ Culture

Enucleated bovine eyes (whole globes) were obtained from VisionTech, Inc. (Mesquite, Texas) immediately post-mortem. Ocular surfaces were disinfected by immersion in a 50% Betadine solution and then rinsed with sterile PBS containing penicillin/streptomycin and amphotericin. Individual globes were placed on a petri dish and a three-step surgical procedure similar to that used by Evans *et al.*³⁶ was used to create a stromal pocket. First, the corneal surface was lightly marked using an 12 mm diameter trephine punch, and the corneal epithelium within the circular area was debrided by scraping, leaving the basement membrane exposed. Next, a 6 mm diameter trephine was used to make a superficial keratotomy groove approximately 150–200 microns deep centrally within the debrided area. Finally, the base of the keratotomy groove was manually expanded approximately 1.5 mm towards the limbus, creating an interlamellar pocket within the stroma.

Following wounding, the wound bed was swabbed and rinsed with sterile culture medium to remove any loose cellular debris. Two series of corneas were prepared. The first series was implanted immediately with hydrogel lenticules (either collagen-modified or unmodified) that were tucked into the expanded pocket of each cornea concealing the lenticule edges within the pocket and exposing 6 mm diameter of the lenticule surface for re-epithelialization. The collagen-modified hydrogels were reacted with 0.3% collagen type I as described in the Materials and Methods section. In the second series of corneas, identical wounds were made but not implanted with lenticules, creating a series of sham wounds which exposed 6 mm diameter of the natural wound bed surface for re-epithelialization. Three samples of sham and hydrogel-implanted samples were set up for each of the 4 time points (t = 0, t = 3 days, t = 5 days, t = 7 days).

The organ culture system used in this study is a modification of that published by Foreman *et al.*³⁷ and later by Evans *et al.*³⁶ and features an air-liquid interface over the cornea. Following wounding and implantation, the corneas (sham and implanted) were excised from the eyes with a 5 mm scleral rim intact and transferred directly onto individual pre-formed agar plugs that provided support and maintained corneal curvature during the culture period. Agar plugs were prepared using a 1:1 mixture of double strength serum-free medium with additives (see below) and 2% agar (Bacto-Agar from Difco, Australia) in distilled water. This mixture was allowed to gel in molds created by inverting previously excised bovine corneas. Wounded corneas on their agar plugs were placed in individual petri dishes with 5 ml complete serum-free culture medium, which was sufficient to bring the medium to the level of the scleral rim. The culture medium used throughout was Dulbecco's Modification of Eagles Medium/Ham's F-12 containing 20 mM L-glutamine (ICN Biomedicals, USA) with 120 mg/ml Penicillin G, 200 mg/ml Streptomycin sulphate, 5 mg/ml Amphotericin B and ITS Premix (Collaborative Biomedical Products, Becton Dickinson, USA) to a final concentration of 5 mg/ml of insulin and transferrin and 5 ng/ml of selenous acid. Samples

were incubated at 37°C in 5% CO₂ in air with once daily medium changes and washes over the corneal surface to remove desquamating epithelial cells from the anterior ocular surface.

The healing process in both sham and implanted corneas maintained in organ culture was evaluated clinically from zero time (freshly wounded) until day 7. Clinical observations of individual corneas were made twice daily during the 7-day period using an epi-illuminated binocular microscope, and the migration of the corneal epithelium over the wound bed or polymer lenticule was charted and photographed using fluorescein (FUL-GLO Barnes Hind from Akorn Inc., Arbita Springs, LA) to stain areas that were not covered by epithelium.

2.8 Surgical Implantation

To test whether the cell culture, bioactivity, and organ culture data translate to surface epithelialization *in vivo*, we performed a limited number of animal studies using the collagen-modified hydrogels that were reacted with 0.3% collagen type I. All animal studies conducted were approved by the Administrative Panel on Laboratory Animal Care of Stanford University, and were in compliance with the Association for Research in Vision and Ophthalmology (ARVO) statement on the use of animals in ophthalmic research. Four adult New Zealand Red rabbits, weighing 3.5 kg – 5.5 kg, were used (1 eye each).

Anesthesia was induced by intramuscular injections of ketamine, xylazine, and glycopyrrolate (35 mg/kg, 5 mg/kg, and 0.02 mg/kg, respectively), and surgeries were performed on the left eye of each rabbit. Once the rabbits were anesthetized, proparacaine ophthalmic solution was given topically. The lid margins and the surrounding periorbital area were cleaned with 10% iodine diluted 50:50 with BSS. Sterile surgical drapes were then placed over the upper and lower eyelids of the left eye. The handle tip of a sterile, disposable scalpel was inserted into the temporal aspect of the lower conjunctival fornix. Using a delicate scooping motion, with manual counter-pressure at around the 12 o'clock position of the eye, the entire globe was proptosed slightly out of the orbit. A 0-silk suture was tied posterior to the equator to maintain position of the globe. Balanced salt solution was continually dropped on the cornea to prevent drying. After adequate positioning of the microsuction ring, a Hansatome microkeratome (Bausch & Lomb, Rochester, NY) was used to create an 8.5 mm diameter, 160 µm thick, laser *in situ* keratomileusis (LASIK) flap. Because of the small size of the rabbit eyes, downward pressure was applied on the entire suction ring apparatus during the passage of the microkeratome motor in order to maintain suction pressure and smooth passage of the motor head. The flap, which was created with a superior hinge, was lifted using a LASIK flap spatula. It was then laid down over the spatula, and a sterile, 1.5 mm-diameter biopsy punch was used to create a hole in its center. A 3.5 mm button of PEG/PAA hydrogel was placed on the stroma. A drop of Neomycin, Polymyxin B, and Dexamethasone combination drops (Maxitrol; Alcon, Ft. Worth, TX) was put on the stromal bed before flap closure. The flap was replaced with the central hole directly over the center of the hydrogel, and adhesion was facilitated around the implant by using a squeegee action with a wet Merocel sponge over the corneal surface. The LASIK flap was allowed to adhere for 5 min. The flap was then checked for good adherence to the underlying stroma. Five, interrupted, 50% thickness, 10–0 nylon sutures were placed radially at the flap-corneal junction. The 0-silk suture was removed, and the globe was gently pushed back into the orbit. Two drops of Maxitrol were administered postoperatively. A tarsorrhaphy was performed with 6–0 silk sutures.

2.9 Follow-up and Clinical Evaluation

Two drops of Maxitrol were given to all rabbits in the operated eyes three times per day for 7 days. The tarsorrhaphy sutures were removed on post-operative day (POD) 2, and corneal sutures were removed on POD 5. Clinical examinations were carried out every 2 days with

the aid of a surgical microscope (Carl Zeiss, Dublin, CA) until termination. These evaluations included observation of the degree of conjunctival injection, quality and stability of the LASIK flap, position of hydrogel disc, health of overlying epithelium (with and without fluorescein dye), and health and clarity of the central and peripheral cornea surrounding the implant.

Histological analysis was done on three rabbits: two at POD 7 and one at POD 14. One of the rabbits intended for a 14-day implantation period extruded the implant at POD 9. The rabbits were euthanized with a lethal dose (2–3 ml) of pentobarbital and phenytoin (Beuthanasia; Schering Plough Animal Health) administered intravenously through the marginal ear vein. Eyes from all animals were enucleated and immediately placed in 2.5% glutaraldehyde/2% paraformaldehyde fixative for histological processing.

2.10 Histological Processing and Evaluation

Initially, the entire globes were fixed in glutaraldehyde for 30 min to maintain the natural curvature of the corneas. The rabbit corneas were then cut away from the rest of the globe using corneal surgical scissors, and then further fixed for 18–24 h. Fresh stock-fixative was prepared for each specimen and its pH was adjusted to 7.2. Cornea samples were then processed using a modified glycol methacrylate protocol (Technovit 7100; EMS, Hatfield, PA), which was successful in preserving the high water content, pH-sensitive PEG/PAA hydrogel through the histological processing stages³⁸.

Thin sections (2–4 μm) were taken and prepared for light microscopy. These sections were assessed for the position of the hydrogel button in relation to the overlying flap, quality and thickness of corneal epithelium, and the presence of an inflammatory response or fibroblastic reaction to the hydrogel.

3. RESULTS

3.1. Synthesis and Swelling of Hydrogels

The synthesized hydrogels were optically clear and could be handled easily with forceps. The hydrogels used for the cell seeding and surface characterization experiments were approximately 500 μm thick and 12.0 mm in diameter. For *in vivo* implantations, thin hydrogel sheets approximately 100 μm -thick were synthesized and cut into small (3.5 mm-diameter) discs. The hydrogels had a water content of 90%.

3.2 Surface Modification

Visualization of FITC-labeled collagen coupled to the PEG/PAA hydrogel demonstrated that the protein binding was discrete and distributed over the entire reacted region (Figure 3). While there were some areas that fluoresced more intensely, there did not appear to be any regions on the hydrogel where collagen binding was not achieved. Quantitative amino acid analysis of total amino acid content showed that the amount of collagen present on the hydrogel was proportional to the amount of collagen reacted to the surface of the NHS-functionalized PEG/PAA IPNs. Three reactions were carried out with three dilutions (0.3%, 0.1%, and 0.03% w/v) of collagen relative to the NHS-functionalized surface, and triplicate analyses were done for each reaction. The amount of protein was determined by the total number of amino acids hydrolyzed from the hydrogel surface (Table 1), while collagen was identified by the presence of characteristic hydroxyproline and proline residues. The baseline measurement of unmodified hydrogels (not shown) revealed no hydroxyproline or proline residues and an amino acid content of less than 0.14 $\mu\text{g}/\text{cm}^2$ (not shown), likely due to sample contamination during handling and transfer. The detected protein content on the surface-modified hydrogels ranged from 44 $\mu\text{g}/\text{cm}^2$ to about 60 $\mu\text{g}/\text{cm}^2$ depending on the

concentration of collagen used. There was not a statistically significant difference among the three reaction stoichiometries used.

3.3 Cell Seeding

As shown earlier in Figure 2a–b, the unmodified PEG/PAA hydrogels did not support the growth of the corneal cell line. There was no evidence of attachment or spreading on the surface of the hydrogel. In contrast, the collagen-coupled hydrogels supported attachment and spreading of the vast majority of cells seeded on the surface per high powered field.

3.4 ELISA Surface Bioactivity Assay

Using an ELISA-based bioactivity assay, we were able to detect collagen type I in its native conformation on both microtiter plates (Figure 4) and the PEG/PAA hydrogel surface (Figure 5). In these experiments, a primary antibody was used to detect native collagen type I, followed by a horseradish peroxidase (HRP)-conjugated secondary antibody. Bioactivity was defined as the intensity of the colorimetric signal (at 450 nm) produced by enzymatic activity of HRP on its substrate, o-phenylenediamine dihydrochloride. The assay was effective over approximately a 100-fold order of magnitude, while heat-denatured collagen was not detected due to the use of a conformation-specific primary antibody (Figure 4). The amount of bioactive collagen could be modulated by changing the hydrogel surface reaction conditions. In Figure 5, the bioactivity of collagen type I coupled to PEG/PAA IPN hydrogels is shown for three different collagen solution concentrations that were chemically reacted with the functionalized hydrogel surfaces. Using the standard curve from Figure 4, the reaction with the 0.3% collagen solution yielded a bioactive, tethered collagen density of roughly 100 ng/cm², while the 0.1% and 0.03% yielded bioactive densities that were on the order of 10 ng/cm². In the subsequent organ culture experiments, PEG/PAA hydrogels were reacted with 0.3% collagen type I using the surface functionalization procedure described above.

3.5 Bovine Organ Culture

Table 2 shows that the collagen-modified hydrogels facilitated epithelial wound closure after five days. In contrast, hydrogels without surface modification did not support epithelial wound healing. Sham samples achieved wound closure after 2.5 days. The appearances of the fluorescein-stained implanted corneas after 5 days in organ culture are shown in Figures 6a and 6b. Figure 6a shows strong staining over the unmodified hydrogel implant, indicating that the fluorescein dye was able to stain the stroma due to a lack of an intact epithelium. Figure 6b shows that no fluorescein staining took place in a collagen-tethered hydrogel implant, indicating that the epithelium had been restored and prevented the permeation of the dye.

Examination of explanted hydrogels in the epithelialized sample under a phase contrast microscope revealed a confluent layer of cells on the hydrogel surface (Figure 7). This is consistent with the clinical observation that fluorescein dye was not able to penetrate the corneal surface and stain the stroma, and is indicative of the barrier functionality of the epithelium.

3.6 *In vivo* implantation

The post-operative appearance of the corneal onlay surgery is shown in Figure 8. Clinically, three out of four PEG/PAA hydrogel implants were well tolerated over a 7-day period of the study. One of the implants was extruded due to unknown causes. The corneas of the remaining three rabbits had no signs of infection, inflammation, or neovascularization. There was no increasing conjunctival redness and the epithelium was free from signs of

sloughing or ulceration. Fluorescein staining was applied during post-operative follow-up sessions to monitor epithelial wound healing over the hydrogel. Clinical follow-up also entailed monitoring of health of the rabbit and its corneas to detect any sign of infection or inflammation and administering topical antibiotics and steroids.

3.7 Histology

Histological analysis of the two 7-day implants showed no evidence of epithelialization (not shown). The implant was present within the corneal stroma without evidence of inflammation, edema, or infection. In contrast, the 14-day implant showed evidence of epithelialization, also in the absence of inflammation, edema, or infection. Light microscopy indicated an intact hydrogel beneath a perforated LASIK flap, with epithelial cells migrating directly onto the surface of the hydrogel implant at day 14 (Figures 9a-b). The epithelium was disorganized but had multiple cell layers, indicating that epithelial wound healing was still in progress and not yet complete. Keratocytes were distributed normally within the collagen fibers directly beneath the implant, with no specific grouping in its vicinity. Consistent with our previous findings in corneal inlay studies³⁹, the absence of immune cells and neovascularization within corneal tissue in all three specimens showed histological tolerance of the PEG/PAA hydrogel implant in the eye.

4. DISCUSSION

Collagen type I is the predominant extracellular matrix protein in the cornea and has been shown to be a promoter of epithelialization *in vivo*²². Photochemical patterning methods allow the localization of reactive groups on the surface of a polymer, and in turn facilitate the formation of a concentrated layer of protein that acts like a basement membrane for attaching cells. Using photoreactive, azide-active-ester linkages developed by Matsuda and coworkers^{33–35}, we have covalently tethered collagen type I to the surfaces of PEG/PAA hydrogels. Our results indicate that azide-active-ester photochemical coupling technique is effective at binding a large amount of collagen type I to the hydrogel, while retaining sufficient bioactivity for the adhesion and growth of corneal epithelial cells.

Quantitative amino acid analysis combined with the ELISA bioactivity results provides two types of information. The former provides quantitative data on the amount of collagen protein attached to the hydrogel surface; this was found to be relatively high (between 40–60 $\mu\text{g}/\text{cm}^2$), indicating that the photochemical tethering strategy is effective and reproducible. The ELISA bioactivity assay yields information about the conformation of the collagen accessible at the hydrogel surface. We defined bioactivity as retention of the protein's native conformation based on the assumption that denatured collagen is ineffective at mediating cell adhesion. Visualization of FITC-labeled collagen confirmed that the deposited collagen was well-distributed over the large reacted region (diameter = 25.0 mm), indicating that uniform photochemical functionalization with active N-hydroxysuccinimide (NHS) ester groups was achieved on the surface.

The strategy employed in this paper enables the covalent coupling of a high amount of bioactive collagen type I. This surface-modification strategy differs from that of Bi *et al.*¹⁶ in that it features a relatively short and rigid tether. Bi and coworkers used an intervening PEG spacer arm and carbodiimidazole chemistry to attach a variety of proteins and polypeptides to poly(hydroxyethyl methacrylate)-based copolymers^{16,40}. Although they found that the absolute amounts of attached proteins were relatively low, they were able to achieve robust cell growth on their tethered surfaces^{15,40}.

Because the exact molecular weight of the collagen we used is unknown, controllable stoichiometry with an azide-active-ester strategy is difficult, if not impossible. The existence

of multiple lysines within collagen, coupled with the high density of reactive NHS groups deposited on the hydrogel, makes it feasible that collagen is attached to the hydrogel surface at multiple sites along its backbone. We hypothesized that this could lead to differences in the bioactivity of the bound collagen layer. To investigate this, we used two quantitative techniques to determine whether any differences could be observed in the bound collagen through alteration of the reaction conditions. The quantitative amino acid analysis yielded an order of magnitude larger amount of collagen ($\sim 40 - 60 \mu\text{g}/\text{cm}^2$, Table 1) than did the ELISA assay ($\sim 100 \text{ ng}/\text{cm}^2$, Figures 4–5) for the three concentrations of collagen used in the coupling reaction. This is most likely because the ELISA assay only probes the outermost, accessible layer of collagen, and only detects collagen in its “bioactive” native conformation. In other words, most of the bound collagen that is beneath the outermost surface, in addition to the denatured collagen on the outermost surface, is not detectable by the conformation-specific antibody used in the ELISA. The fact that the quantitative amino acid analysis showed that the three reacted collagen concentrations (0.03%, 0.1% and 0.3%) yielded similarly large amounts of bound collagen on each of the surfaces indicates that the differences observed in the ELISA assay are due to variations in protein conformation rather than total protein deposition.

In light of these results, we hypothesize that the technique we have used to deposit collagen on the hydrogel surface yields a thick matrix of collagen on the surface with concentration-dependent surface bioactivity. The higher concentration of reacted collagen may lead to a more rapid deposition of a physical matrix on the hydrogel surface with a preponderance of collagen in its native, bioactive conformation on the outermost surface. In contrast, when the lower concentrations are used, the deposition process leads to a matrix of comparable total protein content, but with a less bioactive outer surface. The process that leads to these differences is not clear, but may be related to our hypothesis that binding at multiple sites along the collagen backbone may disrupt its conformation, the structure of the deposited matrix that is formed, and the bioactivity of the surface.

For *in vivo* success of an artificial cornea, a rapid rate of epithelialization and tissue integration is important for anchorage of the device as well as the prevention of microbial contamination post-operatively. The organ culture experiments show that the modification strategy and the resulting high bioactivity of the hydrogel surface yield a material that supports epithelial wound healing, but that this healing takes approximately twice as long as sham wounds. This may be due to a number of factors. First, antimicrobial agents within the hydrogel may have an adverse effect on the migrating cells. Second, collagen type I alone may not be the optimum surface for rapid wound healing. The natural basement membrane consists of collagen type I and IV, laminin, growth factors, as well as fibronectin when in the injured state. Other investigators have demonstrated that combinations of proteins elicit a favorable epithelialization response⁴⁰. Finally, the surgical method produces a situation in which the wound healing surface is “tiered”. Initially, the epithelial cells move across the bare basement membrane on the 1.5 mm stromal rim, and then encounter a steep “drop off” at the edge of the stromal rim before moving into the central hydrogel region. This unnatural terrain is likely to create difficult topography upon which the epithelium tries to heal, leading to a longer time for wound closure and restoration of barrier function. While the implantation procedure and lenticule dimensions were used for screening purposes, if applied as a device such as a corneal onlay, attention should be given to shaping the implant and/or cornea in such a way that a smoother physical transition is provided at the tissue-implant interface.

Based on the successful surface bioactivity assays performed *in vitro*, a small number of animal studies were done to assess the hydrogel’s capacity for surface epithelialization *in vivo*. The modified LASIK surgical implantation method used was done to create a similar

ocular environment as that created in the bovine organ culture studies. Use of a microkeratome to create a flap greatly reduces the amount of trauma and pressure placed on the eye than does the manual dissection process used in the organ culture. Creating a hole in the center of the flap and then laying the flap over the polymer yield a wound similar to that made in the bovine corneas for the organ culture studies. The small size used for the opening (1.5 mm diameter) was for screening purposes only, and may overestimate the actual performance of the hydrogel in supporting epithelialization, since in an actual device, the wound diameter would be 6.0 mm or more.

The results demonstrated that the bioactive collagen-tethered PEG/PAA hydrogels are able to support epithelial overgrowth directly on the hydrogel surface. However, this growth does not occur as quickly as in a normal epithelial wound, which heals in 2–3 days. Epithelial coverage and restoration of barrier function (as shown by fluorescein staining) on the collagen-modified hydrogel require approximately 14 days; however, full epithelialization likely requires an even longer time interval. This apparent delay in wound healing is consistent with the organ culture results, which showed delayed epithelial overgrowth on the hydrogel (5 days) when compared with the sham wound (2.5 days). The reasons for this delay are likely to be multifactorial. In addition to the potential negative effect of antimicrobials diffusing out of the hydrogel on the epithelium described for the organ culture studies, a live rabbit cornea represents a challenging environment for growth over a corneal onlay. Dry-eye is a known complication after LASIK surgery; thus, making a LASIK flap in the rabbit cornea is likely to yield a drier ocular surface and retard the re-epithelialization process. Irritation associated with the wound, from the removal of the central stroma and epithelium, to the flap sutures and the irregular topography of the ocular surface due to the presence of the implanted hydrogel could have all led to a harsh local environment that obstructs the epithelialization process. Because only partial (50%) tarsorrhaphies were done after surgery, excessive blinking or possible rubbing of the eye were still possible post-operatively, which could lead to a situation where the migrating epithelium is regularly sloughed off during the first week or more. In addition, it is feasible that the cell-implant adhesion is low enough at day 7 that histological processing caused removal of any epithelium that may have been present on the hydrogel surface. However, the most likely explanation for suboptimal growth is that the collagen-modified hydrogel does not fully mimic the corneal basement membrane, which in turn precludes rapid, robust epithelialization on its surface.

Nevertheless, the clear presence of migrating epithelium on the PEG/PAA hydrogel at day 14 demonstrates that epithelialization is supported by the collagen-tethered hydrogels. This result supports the *in vitro* characterization presented in this paper, which indicated that the azide-active-ester surface modification strategy for linking collagen to the hydrogel is successful in creating a bioactive matrix upon which epithelial cells can grow under an air-liquid interface in organ culture. Further work will be directed toward identifying the reasons for the time-delay in epithelialization and addressing ways in which the wound healing process can not only be accelerated, but also optimized from both a morphological and functional standpoint. Fabricating hydrogel lenticles with tapered edges will certainly be important for creating a smooth ocular surface and transition between stroma and implant. Moreover, incorporation of other extracellular matrix proteins and/or growth factors onto the hydrogel surface may yield more robust or rapid epithelial migration and proliferation.

5. CONCLUSIONS

This paper describes the development and characterization of collagen-coupled poly(ethylene glycol)/poly(acrylic acid) (PEG/PAA) interpenetrating polymer network

hydrogels. Quantitative amino acid analysis and FITC-labeling of collagen were used to determine the amount and distribution of collagen on the surface of the hydrogels. The bioactivity of the coupled collagen was detected by a conformation-specific antibody and was found to vary with the concentration of collagen reacted to the photochemical functionalized hydrogel surfaces. A wound healing assay based on an organ culture model demonstrated that this bioactive surface supports epithelial wound closure over the hydrogel but at a decreased rate relative to sham wounds. Implantation of the hydrogel into the corneas of live rabbits demonstrated that epithelial cell migration is supported by the material, although the rate of migration and morphology of the epithelium were not normal. The results from the study will be used as a guide toward the optimization of bioactive hydrogels with potential in corneal implant applications such as a corneal onlay and an artificial cornea.

Acknowledgments

This research was supported by the Bio-X Interdisciplinary Initiatives Program and Bio-X Graduate Student Fellowship at Stanford University and the Office of Technology Licensing at Stanford University. Additional external support was also received from VISX, Incorporated (now VISX Technology) and the Fight for Sight Foundation. The authors thank Ilya Kucher at the Molecular Structure Facility at UC Davis for conducting the quantitative amino acid analyses.

References

1. Carlsson DJ, Li F, Shimmura S, Griffith M. Bioengineered corneas: how close are we? *Curr Opin Ophthalmol* 2003;14(4):192–7. [PubMed: 12888716]
2. Chirila TV. An overview of the development of artificial corneas with porous skirts and the use of PHEMA for such an application. *Biomaterials* 2001;22(24):3311–7. [PubMed: 11700803]
3. Duan D, Klenkler BJ, Sheardown H. Progress in the development of a corneal replacement: keratoprotheses and tissue-engineered corneas. *Expert Review of Medical Devices* 2006;3(1):59–72. [PubMed: 16359253]
4. Griffith M, Hakim M, Shimmura S, Watsky MA, Li F, Carlsson D, Doillon CJ, Nakamura M, Suuronen E, Shinozaki N, et al. Artificial human corneas: scaffolds for transplantation and host regeneration. *Cornea* 2002;21(7 Suppl):S54–61. [PubMed: 12484700]
5. Li F, Carlsson D, Lohmann C, Suuronen E, Vascotto S, Kobuch K, Sheardown H, Munger R, Nakamura M, Griffith M. Cellular and nerve regeneration within a biosynthetic extracellular matrix for corneal transplantation. *Proc Natl Acad Sci U S A* 2003;100(26):15346–51. [PubMed: 14660789]
6. Khan B, Dudenhofer EJ, Dohlman CH. Keratoprosthesis: an update. *Curr Opin Ophthalmol* 2001;12(4):282–7. [PubMed: 11507341]
7. Peralta RJ, Kanellopoulos AJ. Boston Keratoprosthesis : A Long-Term Prospective Clinical Study. *Invest Ophthalmol Vis Sci* 2007;48 E-Abstract 1895.
8. Alio JL, Mulet MR, Haroun H, et al. Five year follow-up of biocolonisable microporous fluorocarbon haptic (BIOKOP) keratoprosthesis implantation in patients with high risk corneal graft failure. *British Journal of Ophthalmology* 2004;88:1585–1589. [PubMed: 15550368]
9. Kim MK, Lee JL, Wee WR, Lee JH. Seoul-type keratoprosthesis: preliminary results of the first 7 human cases. *Arch Ophthalmol* 2002;120:761–766. [PubMed: 12049581]
10. Doane MG, Dohlman CH, Bearn G. Fabrication of a keratoprosthesis. *Cornea* 1996;15(2):179–184. [PubMed: 8925666]
11. Ilhan-Sarac O, Akpek EK. Current concepts and techniques in keratoprosthesis. *Current Opinion in Ophthalmology* 2005;16:246–250. [PubMed: 16000898]
12. Chirila TV, Hicks CR, Dalton PD, Vijayasekaran S, Lou X, Anthony YH. Artificial Cornea. *Progress in Polymer Science* 1998;23(3):447–473.

13. Ricci R, Pecorella I, Ciardi A, Della Rocca C, Di Tondo U, Marchi V. Strampelli's osteo-odonto-keratoprosthesis. Clinical and histological long-term features of three prostheses. *Br J Ophthalmol* 1992;76(4):232–4. [PubMed: 1390492]
14. Polack FM, Heimke G. Ceramic keratoprosthesis. *Ophthalmology* 1980;87(7):693–8. [PubMed: 7402597]
15. Wallace C, Jacob JT, Stoltz A, Bi JJ, Bundy K. Corneal epithelial adhesion strength to tethered-protein/peptide modified hydrogel surfaces. *Journal of Biomedical Materials Research Part A* 2005;72A(1):19–24. [PubMed: 15534866]
16. Bi JJ, Downs JC, Jacob JT. Tethered protein/peptide-surface-modified hydrogels. *Journal of Biomaterials Science-Polymer Edition* 2004;15(7):905–916. [PubMed: 15318800]
17. Bi JJ, Rochefort J, Jacob JT. Corneal epithelial cell growth over surface-modified hydrogels. *Investigative Ophthalmology & Visual Science* 2001;42(4):S267–S267.
18. Klenkler BJ, Griffith M, Becerril C, West-Mays JA, Sheardown H. EGF-grafted PDMS surfaces in artificial cornea applications. *Biomaterials* 2005;26(35):7286–7296. [PubMed: 16019066]
19. Merrett K, Griffith CM, Deslandes Y, Pleizier G, Sheardown H. Adhesion of corneal epithelial cells to cell adhesion peptide modified pHEMA surfaces. *J Biomater Sci Polym Ed* 2001;12(6):647–71. [PubMed: 11556742]
20. Evans MD, Xie RZ, Fabbri M, Madigan MC, Chaouk H, Beumer GJ, Meijs GF, Griesser HJ, Steele JG, Sweeney DF. Epithelialization of a synthetic polymer in the feline cornea: a preliminary study. *Invest Ophthalmol Vis Sci* 2000;41(7):1674–80. [PubMed: 10845584]
21. Dalton BA, Walboomers XF, Dziegielewski M, Evans MD, Taylor S, Jansen JA, Steele JG. Modulation of epithelial tissue and cell migration by microgrooves. *J Biomed Mater Res* 2001;56(2):195–207. [PubMed: 11340589]
22. Sweeney DF, Xie RZ, Evans MD, Vannas A, Tout SD, Griesser HJ, Johnson G, Steele JG. A comparison of biological coatings for the promotion of corneal epithelialization of synthetic surface in vivo. *Invest Ophthalmol Vis Sci* 2003;44(8):3301–9. [PubMed: 12882774]
23. Gipson IK, Inatomi T. Extracellular matrix and growth factors in corneal wound healing. *Curr Opin Ophthalmol* 1995;6(4):3–10. [PubMed: 10150880]
24. Griffith, M.; Watsky, MA.; Liu, CY.; Randall, VT. Epithelial Cell Culture: Cornea. In: Atala AA, RP., editor. *Methods of Tissue Engineering*. San Francisco: Academic Press; 2002. p. 131-140.
25. Gong JP, Katsuyama Y, Kurokawa T, Osada Y. Double-network hydrogels with extremely high mechanical strength. *Advanced Materials* 2003;15(14):1155–1158.
26. Myung D, Koh W, Ko J, Hu Y, Carrasco M, Noolandi J, Ta CN, Frank CW. Biomimetic strain hardening in interpenetrating polymer network hydrogels. *Polymer* 2007;48:5376–5387.
27. Myung D, Koh W, Bakri A, Zhang F, Marshall A, Ko J, Noolandi J, Carrasco M, Cochran JR, Frank CW, et al. Design and fabrication of an artificial cornea based on a photolithographically patterned hydrogel construct. *Biomed Microdevices*. 2007
28. Myung D, Koh W, Ko J, Noolandi J, Carrasco M, Smith A, Frank C, Ta C. Characterization of poly(ethylene glycol) and poly(acrylic acid) double networks for corneal implant applications. *Invest Ophthalmol Vis Sci* 2005;46 E-Abstract 5003.
29. Nguyen KT, West JL. Photopolymerizable hydrogels for tissue engineering applications. *Biomaterials* 2002;23(22):4307–14. [PubMed: 12219820]
30. Czeslik C, Jackler G, Hazlett T, Gratton E, Steitz R, Wittemann A, Ballauff M. Salt-induced protein resistance of polyelectrolyte brushes studied using fluorescence correlation spectroscopy and neutron reflectometry. *Physical Chemistry Chemical Physics* 2004;6:5557–5563.
31. Cruise GM, Scharp DS, Hubbell JA. Characterization of permeability and network structure of interfacially photopolymerized poly(ethylene glycol) diacrylate hydrogels. *Biomaterials* 1998;19(14):1287–94. [PubMed: 9720892]
32. Murata H, Chang BJ, Prucker O, Dahm M, Ruhe J. Polymeric coatings for biomedical devices. *Surface Science* 2004;570(1–2):111–118.
33. Matsuda T, Sugawara T. Photochemical Protein Fixation on Polymer Surfaces Via Derivatized Phenyl Azido Group. *Langmuir* 1995;11(6):2272–2276.
34. Matsuda T, Inoue K, Sugawara T. Development of micropatterning technology for cultured cells. *ASAIO Transactions* 1990;36(3):M559–62. [PubMed: 2252750]

35. Matsuda T, Sugawara T. Development of surface photochemical modification method for micropatterning of cultured cells. *J Biomed Mater Res* 1995;29(6):749–56. [PubMed: 7593012]
36. Evans MD, McFarland GA, Xie RZ, Taylor S, Wilkie JS, Chaouk H. The use of corneal organ culture in biocompatibility studies. *Biomaterials* 2002;23(5):1359–67. [PubMed: 11808538]
37. Foreman DM, Pancholi S, Jarvis-Evans J, McLeod D, Boulton ME. A Simple Organ Culture Model for Assessing the Effects of Growth Factors on Corneal Re-epithelialization. *Experimental Eye Research* 1996;62(5):555–564. [PubMed: 8759523]
38. Farooqui N, Myung D, Masek M, Dalal R, Koh W, Gupta S, Noolandi J, Frank C, Ta CN. Histological Evaluation of Poly(Ethylene Glycol)–Poly(Acrylic Acid) (PEG–PAA) Double Network Hydrogel Corneal Implant. *Invest Ophthalmol Vis Sci* 2005;46 E-Abstract 873.
39. Bakri A, Farooqui N, Myung D, Koh WG, Noolandi J, Carrasco M, Frank C, Ta CN. Biocompatibility of a Hydrogel Corneal Inlay in vivo. *Invest Ophthalmol Vis Sci* 2006;47 E-Abstract 3592.
40. Jacob JT, Rochefort JR, Bi JJ, Gebhardt BM. Corneal epithelial cell growth over tethered-protein/peptide surface-modified hydrogels. *Journal of Biomedical Materials Research Part B-Applied Biomaterials* 2005;72B(1):198–205.

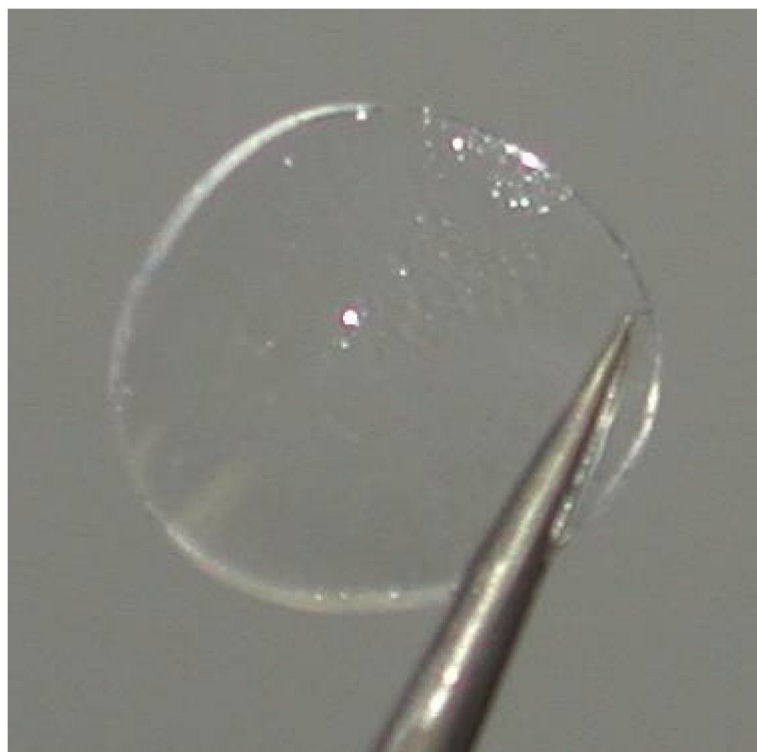


Figure 1. Photograph of a PEG/PAA hydrogel (12.0 mm diameter, ~500 μm thick) used in the surface characterization studies described in this paper.

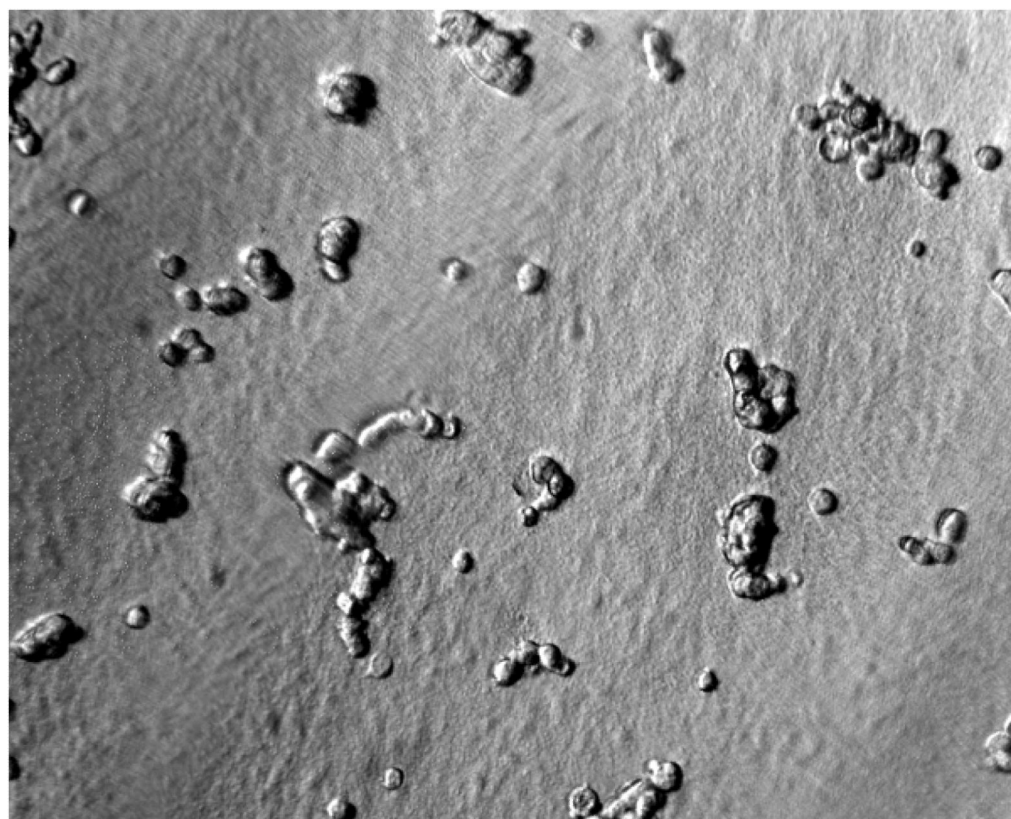


Figure 2.

Figure 2a. PEG/PAA IPN hydrogels are intrinsically resistant to cell growth in culture. Shown here are cells from a corneal cell line (ATCC #CCL60) seeded but not spreading on a PEG/PAA hydrogel after 24 hours.

Figure 2b: Cells from a corneal cell line (ATCC #CCL60) spreading on a PEG/PAA hydrogel photochemically modified with collagen type I, after 24 hours.

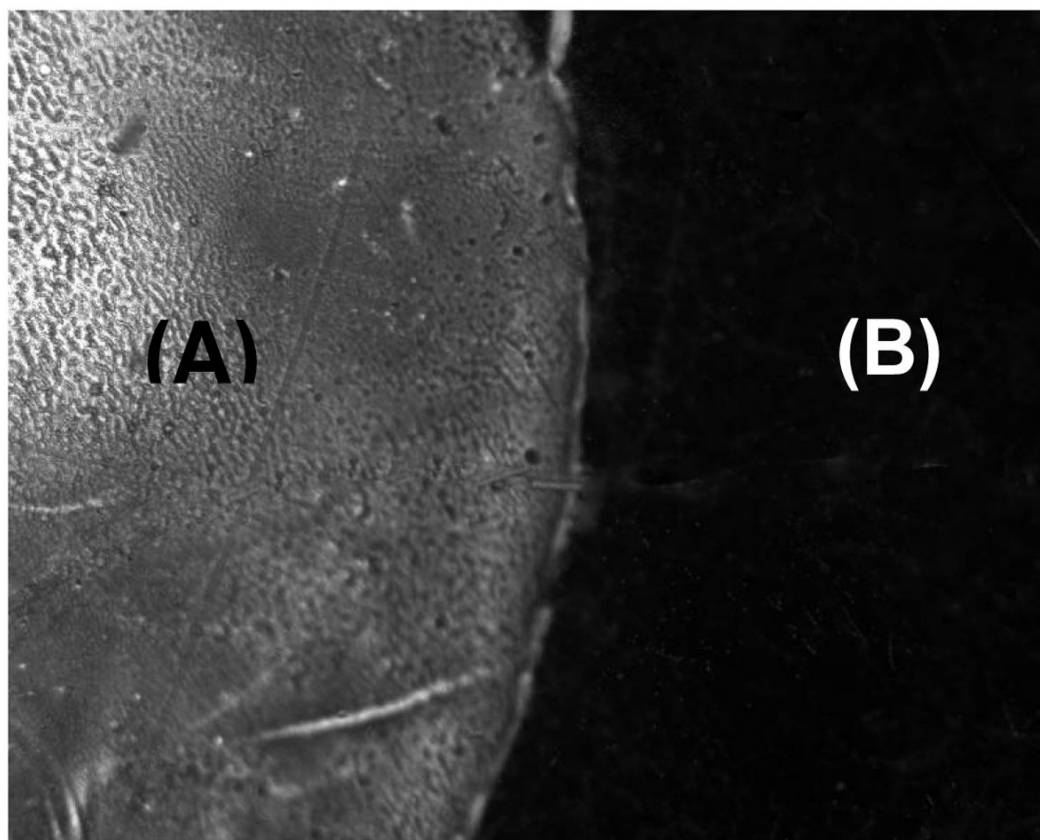


Figure 3. Fluorescent photomicrograph showing FITC-labeled collagen type I bound to a hydrogel surface via amide linkages mediated by azide-active-ester linkages. The region labeled (A) is the portion of the hydrogel that is coupled with FITC-labeled collagen type I, while the dark region labeled (B) is the unmodified region of the hydrogel.

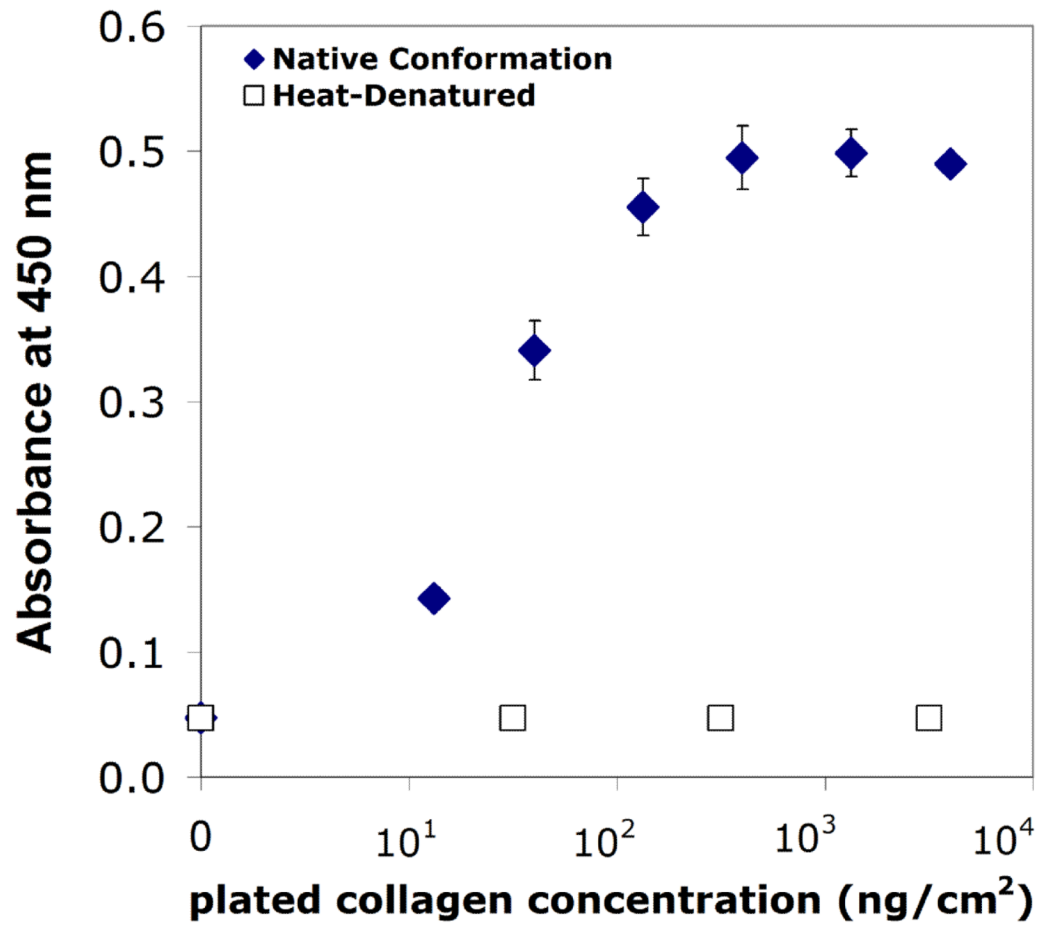


Figure 4. Standard curve of absorbance versus plated collagen concentration for bioactive collagen (solid diamonds) and heat-denatured collagen (open squares).

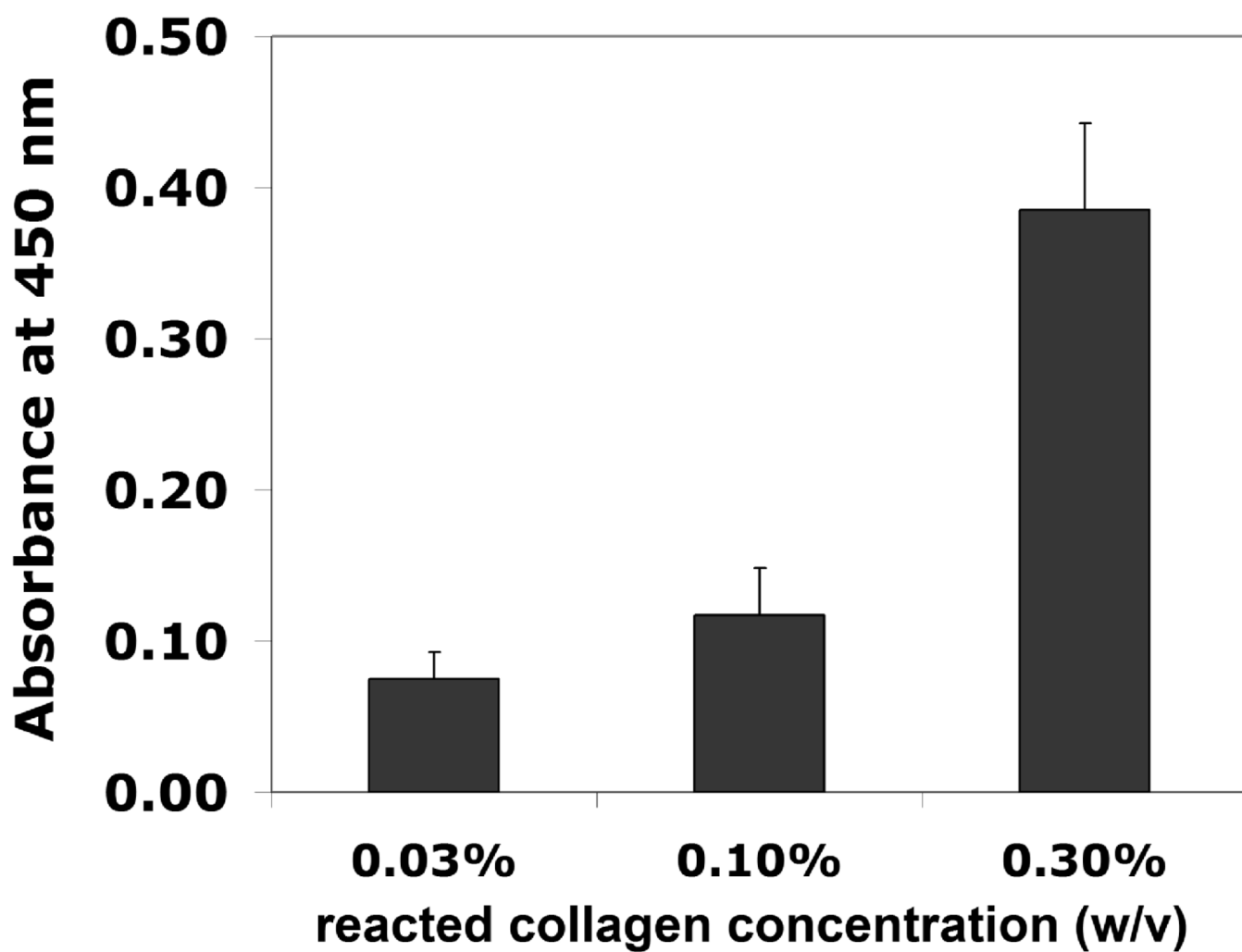


Figure 5. Absorbance readings of the NHS ester-functionalized PEG/PAA hydrogel after reaction with various collagen concentrations.

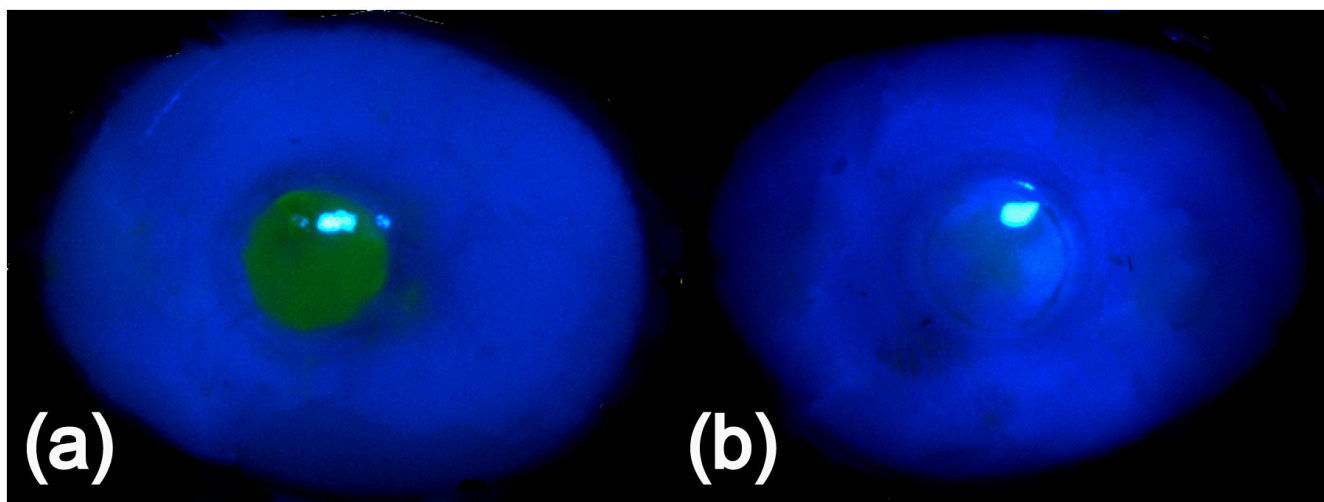


Figure 6.

(a) Appearance of bovine cornea with implanted unmodified PEG/PAA hydrogel after 5 days. The wounded area remained unepithelialized and is stained with fluorescein. **(b)** Appearance of bovine cornea with implanted collagen-tethered PEG/PAA hydrogel after 5 days. The wounded area is epithelialized and does not permit staining with fluorescein dye.

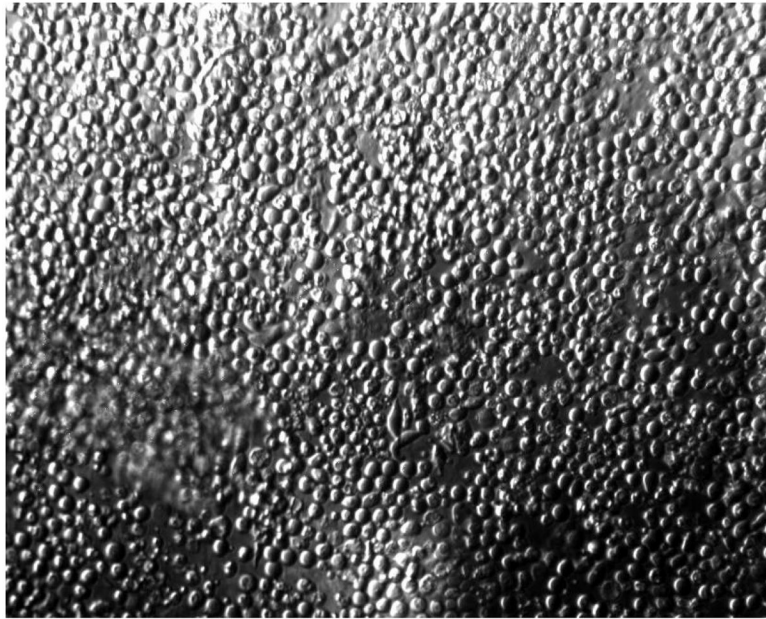


Figure 7. Photomicrograph of a collagen-tethered hydrogel explant after 5 days in organ culture. The explant is covered with a confluent monolayer of epithelial cells. Cross-sectional histology was not obtained, and thus the three-dimensional morphology and existence of multiple layers is unknown.

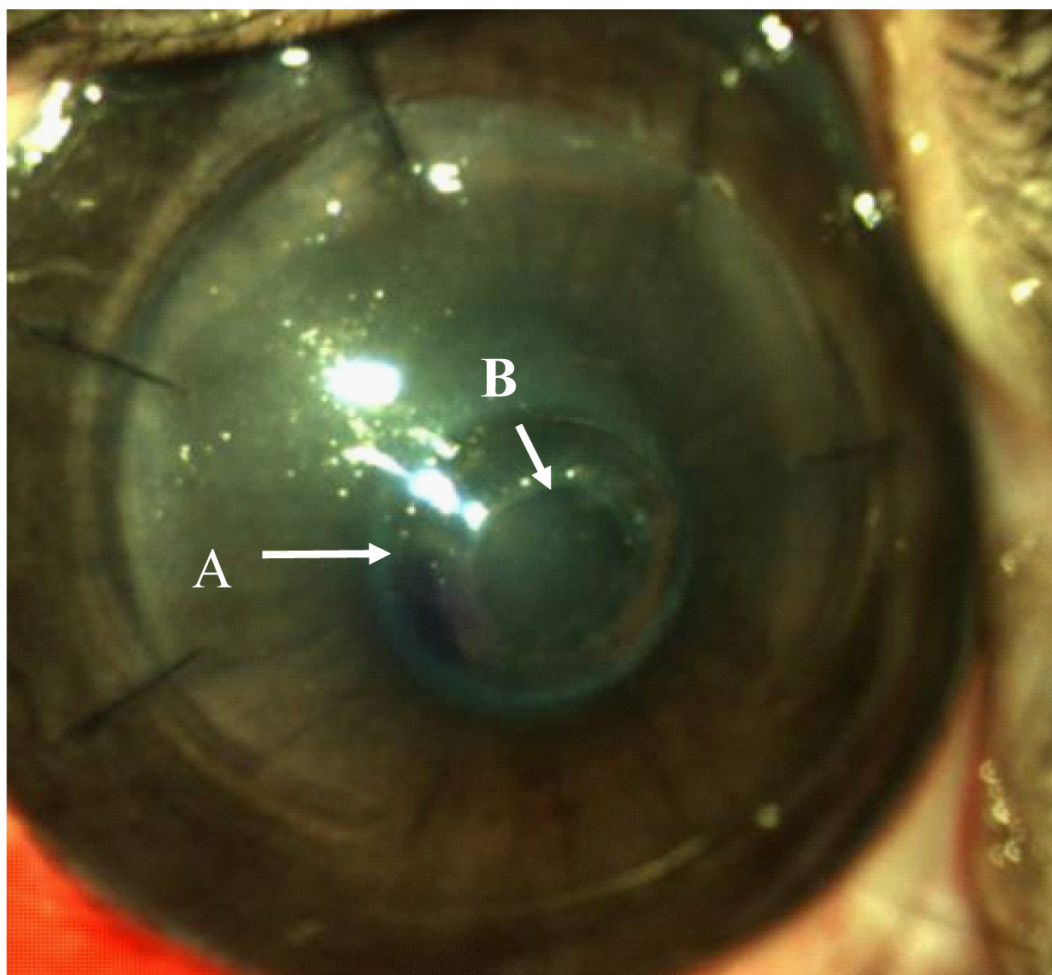
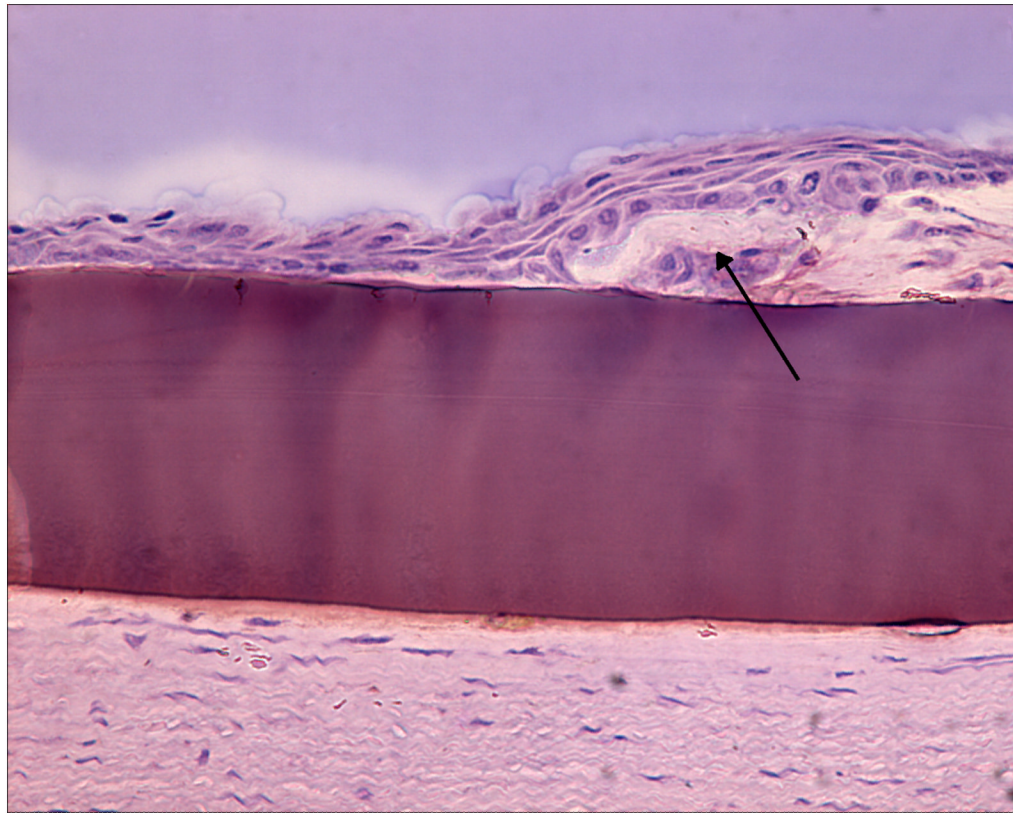


Figure 8. Post-operative appearance of a collagen-tethered hydrogel corneal onlay in a rabbit cornea. Arrow (A) indicates the edge of the hydrogel underneath the LASIK flap, and arrow (B) indicates the edge of the hole in the flap that is placed over the center of the hydrogel.



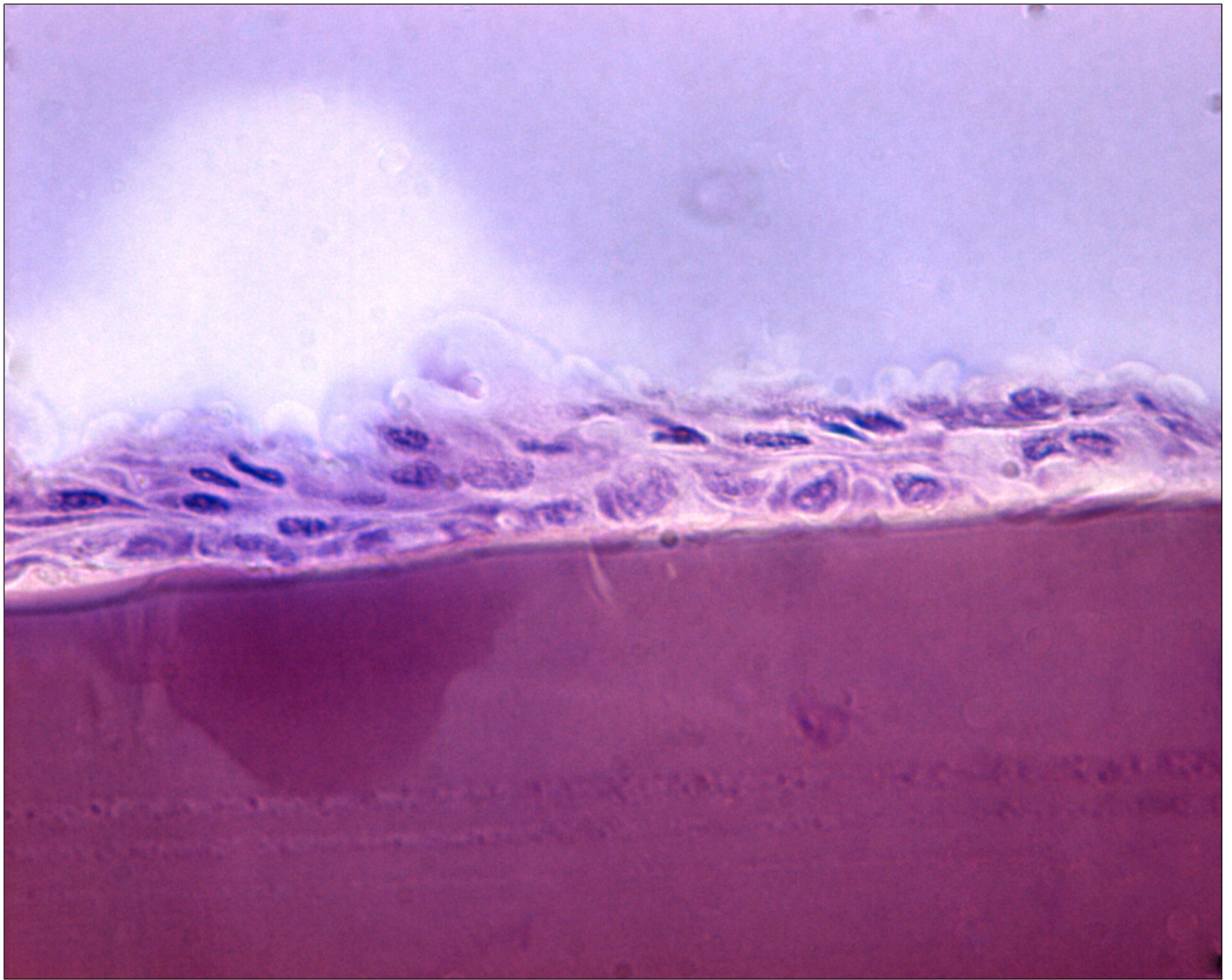
**Figure 9.**

Figure 9a. Histological section showing epithelial overgrowth directly on a PEG/PAA hydrogel (central purple region, 100 microns thick) in the central part of a rabbit corneal onlay after 14 days. The arrow indicates the “ledge” of anterior cornea from which the epithelial cells are migrating.

Figure 9b. A more central, magnified view of the histological section shown in Figure 9a.

Table 1

Results of quantitative amino acid analysis on collagen-tethered PEG/PAA hydrogels (in total micrograms).

Residue	Reaction 1 [*]	Reaction 2 ^{**}	Reaction 3 ^{***}
Asx	3.18 ± 1.01	2.62 ± 0.26	2.37 ± 0.39
Thr	1.36 ± 0.50	1.10 ± 0.10	0.97 ± 0.15
Ser	1.73 ± 0.55	1.40 ± 0.14	1.28 ± 0.19
Glx	8.56 ± 2.75	7.58 ± 0.80	6.90 ± 1.13
Pro	7.62 ± 2.34	6.18 ± 0.74	5.64 ± 0.97
Gly	11.78 ± 3.06	9.75 ± 1.10	8.92 ± 1.48
Ala	4.84 ± 1.47	3.96 ± 0.44	3.60 ± 0.60
Val	1.55 ± 0.50	1.09 ± 0.12	0.93 ± 0.15
Ile	0.90 ± 0.29	0.69 ± 0.06	0.60 ± 0.10
Leu	1.80 ± 0.58	1.38 ± 0.14	1.17 ± 0.19
Tyr	0.18 ± 0.06	0.13 ± 0.01	0.11 ± 0.01
Phe	0.96 ± 0.32	0.77 ± 0.09	0.70 ± 0.12
His	0.52 ± 0.17	0.34 ± 0.04	0.29 ± 0.05
Lys	1.97 ± 0.63	1.70 ± 0.17	1.57 ± 0.25
Arg	4.97 ± 1.62	3.89 ± 0.47	3.52 ± 0.59
Hy Pro	6.80 ± 1.99	5.91 ± 0.71	5.51 ± 0.96
Hy Lys	0.78 ± 0.12	0.63 ± 0.06	0.55 ± 0.09
Total	59.50 ± 17.94	49.13 ± 5.46	44.63 ± 7.42

* Reaction 1 involved incubation of the hydrogels with 0.03% w/v collagen type I

** Reaction 2 involved incubation of the hydrogels with 0.1% w/v collagen type I

*** Reaction 3 involved incubation of the hydrogels with 0.3% w/v collagen type I

Table 2

Wound healing results of implanted and non-implanted bovine corneas in organ culture.

Sample	Surface Modification	Wound Closure Day
Sham = no implant (positive control)	N/A	2.5
Non-Modified PEG-PAA IPN hydrogel	None	No growth by Day 7
Modified PEG-PAA IPN hydrogel	collagen type I via azide- active-ester linkage	5